JCTC Journal of Chemical Theory and Computation

Article

pubs.acs.org/JCTC

Linear Response Theory and Electronic Transition Energies for a Fully Polarizable QM/Classical Hamiltonian

Filippo Lipparini,*[,†] Chiara Cappelli,[†,‡] and Vincenzo Barone[†]

[†]Scuola Normale Superiore, Piazza dei Cavalieri 7, 56126 Pisa, Italy

[‡]Dipartimento di Chimica e Chimica Industriale, Università di Pisa, Via Risorgimento 35, 56126 Pisa, Italy

Supporting Information

ABSTRACT: A fully polarizable quantum/classical Hamiltonian including SCF (HF or DFT), fluctuating charge, and polarizable continuum regions is introduced and implemented for electronic energies of ground and excited states, using, in the latter case, a linear response formulation. After calibration and validation of the approach, preliminary results are presented for pyrimidine in aqueous solution and for retinal in a rhodopsin mimic. The results are consistent with more tested methodologies and pave the route toward fully consistent yet effective simulations of large systems of technological and/or biological interest in their natural environments.

1. INTRODUCTION

Computational strategies to include environmental effects in the modeling of molecular phenomena are, nowadays, valuable tools used to bridge the gap between theory and experiment. It is well-known that the chemical environment, being either a solvent, a solid state matrix, or any other complex molecular system (such as a biological macromolecule), can significantly alter the structural and response properties of some chemically interesting molecular probes. While the increase in computational power, combined with state-of-art linear scaling techniques, has made possible quantum mechanical (QM) calculations on systems composed of several thousands of atoms, a number of problems arising in the description of complex systems cannot be addressed simply by brute-force approaches. As an example, calculations on systems which are not well represented by a single conformer and require statistical averages of the computed properties would lead to an enormous number of barely feasible computations. Not only that, several chemically interesting properties need very accurate computations, which are expensive already for medium-sized systems; to reduce the level of accuracy so to increase the size of treatable systems could yield meaningless or wrong results. Furthermore, such an effort would probably be largely unnecessary when the aim of the calculation is to compute some *local* property, which is almost completely determined by a small portion of the complex system. This is the case, for instance, for spectroscopic properties of chromophores embedded in a biological matrix or in solution.

When the aim of the computation is to describe the properties of small- to medium-sized molecules, taking into account the effect of the chemical environment without being interested in the environment itself, *focused models* represent an excellent strategy: the core of the system can be in fact described at a suitable level of theory, whereas the effects of the surroundings can be included in an averaged or approximate way. In the following, we will use solvation as a case of study and call *solute* the molecular core of our system and *solvent* the remainder. We point out that this definition of solute and solvent needs to be intended in a broad way, as our model is not limited to solvation. Among the various focused models, the so-called QM/MM strategies,[1−10] coupling quantum (QM) and classical (molecular mechanics, MM) approaches, can provide a successful way to describe solvent effects on the molecular structure and properties of the solute. The solvent can be represented by a set of charges reproducing its electrostatic potential, or, in more refined models, by higher terms in the multipolar expansion. To take into account repulsion and dispersion interactions, appropriate empirical potentials can be employed, the most popular being the Lennard-Jones one. This strategy introduces in the molecular Hamiltonian a fixed, external potential which will alter the molecular density in a suitable way: the described approach is usually called *electrostatic embedding*. A further level of refinement is to consider mutual polarization effects between the solute and the solvent by using a *polarizable* force field. This *polarizable embedding* introduces in the molecular Hamiltonian a term depending on the electronic density and requires an iterative solution of the QM equations. Viable embedding approaches have been reviewed by Bakowies and Thiel.[11] Although the polarizable embedding requires in principle the (iterative) solution of nonlinear equations, the structure of self consistent field (SCF) methods—including modern density functional theory (DFT) based Kohn−Sham models—remains unaltered.

QM/MM strategies, however, do not help solve the problem of configuration sampling: in order to reduce the dimension of the system, it is possible to employ continuum models, among which one of the most successful is the polarizable continuum model (PCM).[12−14] A possible limitation of such models is the case of a system dominated by strong and directional specific interactions, such as hydrogen bonding. Continuum and discrete solvation can be successfully combined to produce a methodology where the strengths of one approach compensate

Received: June 19, 2012

dx.doi.org/10.1021/ct3005062 | J. Chem. Theory Comput. XXXX, XXX, XXX−XXX

for the weaknesses of the other. While QM/MM/PCM strategies have been widely employed,[15−23] the first fully polarizable QM/MM/PCM methodology has been presented only recently[20] for a polarizable force field based on Thole's point dipole approximation.[24] A combined polarizable MM/PCM strategy in the framework of classical simulations based on the fluctuating charge (FQ) model[25] has been developed by some of us,[26] where the PCM has been employed to grant a correct handling of the electrostatic interaction for nonperiodic boundary condition (nPBC) simulations.[27−31]

Here, we will present the theory and implementation of a fully polarizable quantum-classical Hamiltonian based on the FQ model possibly combined with the PCM. We will derive working equations for the energy of the ground and excited states in the framework of SCF and linear response theory, also called time-dependent SCF (TD-SCF) theory. A polarizable QM/MM model has already been used to describe excited states[32−38] or more complex phenomena such as electronic energy transfer;[9,39,40] however, to the best of our knowledge, only one implementation of a fully polarizable QM/MM/PCM model exists.[20] Our implementation differs from the aforementioned one as we employ the FQ model to include polarization in the MM layer, while ref 20 resorts to Thole's point dipole method.[24] Furthermore, our formulation is based on a fully variational energy functional in all the degrees of freedom of the multilayer system: electron densities, polarizable charges, and PCM apparent surface charges (ASC).

The paper is organized as follows: In section 2, a variational energy functional is defined, from which coupled SCF/FQ equations are obtained. By making use of its variational formulation, the inclusion of the PCM will be shortly discussed. Finally, our method and other polarizable QM/MM(/PCM) approaches will be compared. In section 3, linear response equations will be derived, followed in section 4 by few test applications. Finally, section 5 gives some conclusions and perspectives.

2. THEORY

Notation. We will use the bold font to indicate vectors and matrices as a whole, while we will use the normal font for their elements. For instance, $\mathbf{P}$ refers to the density matrix, whose elements are $P_{\mu\nu}$. $\mathbf{q}$ is the vector composed of all the FQs, while the ith charge is q_i, and $\mathbf{F}$ is the representation matrix of the Fock operator $\mathcal{F}$ in some basis set, where we use either calligraphic fonts or the $\hat{x}$ accent to denote operators. If a quantity is both a matrix (i.e., with respect to the atomic basis set) and a vector (i.e., with respect to the charges manifold), we will use the bold font when we deal with the whole vector irrespectively of the matrix attribute. As an example, we will denote with $\mathbf{V}_{\mu\nu}$ the vector made of the matrices $V_{\mu\nu,i}$ so that, for instance

$$\mathbf{q}^{\dagger}\mathbf{V}_{\mu\nu} = \sum_i q_i V_{\mu\nu,i}$$

We will use the accent $\sim$ to denote quantities including a FQ contribution: for instance, $\tilde{\mathbf{F}}$ will be the FQ corrected Fock matrix.

In this section, we will recap briefly the fluctuating charge (FQ) model and define its coupling with a QM description of a molecular system at the SCF level of theory. Starting from the electrostatic energy for the FQ model, we will build an energy functional for the QM/classical system assuming that the two portions interact classically. The coupled FQ and Fock or Kohn−Sham (KS) equations will then be derived. We will finally introduce a further coupling with a polarizable continuum, which, as we will show, does not alter the formal structure of the equations.

In the FQ model, polarization effects in the description of a molecular system are introduced by endowing each atom with a charge, whose value depends on a set of parameters and on the chemical environment.[25,41,42] The parameters used to determine these charges are the atomic electronegativities and hardnesses, which can be connected to the first and second derivatives of the molecular energy with respect to the net charge on the atom through the framework of density functional theory.[43,44] While the electronegativities can be viewed as the sources of the FQs, in the sense that differences in atomic electronegativities promote charge separation, the hardnesses are related to the interaction of the charges among themselves, with particular reference to self-interaction: for an insulated atom, the hardness corresponds to the work necessary to create a unit charge on the site. In a molecular context, the charges interact with each other: the equilibrium between those interactions and the differences in the atomic electronegativities acts as a physical basis for the electronegativity equalization principle[43,45] (EEP), which defines the FQ model.

Let $\boldsymbol{\chi}$ be the vector of atomic electronegativities and $\mathbf{J}$ be the interaction kernel for the FQs: the electrostatic energy of the system is

$$E = \sum_{i=1}^{N_q} \left[\chi_i q_i + \eta_i q_i^2 + \sum_{j>i} J_{ij} q_i q_j\right] \tag{1}$$

where the sum runs over the N_q FQs. The choice of the interaction kernel defines different versions of the FQ model:[25,44−59] we will follow Ohno's ansatz,[55] which is the same employed in the CharMM force field[57,58] and in the reactive ReaxFF:[59]

$$J_{ii} = 2\eta_i,\ J_{ij} = \frac{\eta_{ij}}{\left[1 + \eta_{ij}^2 r_{ij}^2\right]^{1/2}} \tag{2}$$

where η_i is the hardness of the ith atom,

$$\eta_{ij} = \frac{\eta_i + \eta_j}{2}$$

is the average of the atomic hardnesses of atoms i and j, and $r_{ij} = |\mathbf{r}_i - \mathbf{r}_j|$ is the distance between two MM atoms. Notice that the modification of the interaction Kernel permits one to employ a different model for the fluctuating charges. In the case of a nonlinear system of equations (e.g., the one that determines the QEq[45] charges), a matrix inversion approach is not viable: iterative techniques are mandatory. Nevertheless, only small changes have to be introduced in the general framework that we will discuss in the following.

The equilibrium charges satisfy the EEP, i.e. they minimize the total energy under a suitable charge conservation constraint. While several models have been proposed to take into account charge transfer among FQ-described molecules,[50,53,60−63] we will not consider such a phenomenon and hence impose charge conservation for each molecule. This can be done by introducing as many Lagrange multipliers as molecules, through the functional

dx.doi.org/10.1021/ct3005062 | J. Chem. Theory Comput. XXXX, XXX, XXX−XXX

$$F(\mathbf{q}, \lambda) = \sum_{\alpha,i} q_{\alpha i}\chi_{\alpha i} + \frac{1}{2}\sum_{\alpha,i}\sum_{\beta,j} q_{\alpha i}J_{\alpha i,\beta j}q_{\beta j} + \sum_{\alpha}\lambda_\alpha\sum_i (q_{\alpha i} - Q_\alpha) = \mathbf{q}^\dagger\chi + \frac{1}{2}\mathbf{q}^\dagger\mathbf{J}\mathbf{q} + \lambda^\dagger\mathbf{q} \quad (3)$$

where the Greek indexes α and β run on molecules and the Latin ones on the atoms of each molecule. The FQs are the solution of the stationary problem:

$$\begin{cases} \sum_{\beta,j} J_{\alpha i,\beta j}q_{\beta j} + \lambda_\alpha = -\chi_{\alpha i} \\ \sum_i q_{\alpha_i} = Q_\alpha \end{cases} \quad (4)$$

or, in a more compact notation:

$$\mathbf{D}\mathbf{q}_\lambda = -\mathbf{C}_Q \quad (5)$$

where the definition of the $\mathbf{D}$ matrix follows from eq 4. More details can be found elsewhere.[26] $\mathbf{C}_Q$ is a vector containing atomic electronegativities and total charge constraints, whereas $\mathbf{q}_\lambda$ is a vector containing charges and Lagrange multipliers. We remark that the $\mathbf{D}$ matrix depends on the relative position of the MM atoms. To make the notation less cumbersome, we will drop the distinction between different molecules in the FQ-related quantities; i.e., we will just use one index per charge, underlying that the constraints are included in the definition of the matrix $\mathbf{D}$.

In the perspective of coupling the FQs to a QM description of the solute, it is worth it to notice that, from a mathematical point of view, the functional eq 3 gives a *variational* tool to describe the MM portion of the system in a self-contained way. If one assumes that the FQs interact with some external source, this interaction is easily introduced by adding to the energy functional the proper interaction potential and then imposing stationary conditions. This means that if the source is an independent (also from the mathematical point of view) part of the system, such as a QM-described molecule, a new, extended functional is to be defined. Such a functional is composed of three terms:

$$\mathcal{E} = E_{QM} + E_{MM} + E_{QM/MM} \quad (6)$$

If the QM term is a variational functional itself, the resulting, coupled equations are derived following the same procedure as for the uncoupled case. We will follow this idea, which has already been proposed to couple the polarizable continuum model (PCM) to a Fock-like Hamiltonian,[64,65] assuming that the QM and MM portions of the system interact classically; that is, the QM density interacts as a classical density of charge with the FQs:

$$E_{QM/MM} = \sum_{i=1}^{N_q} \Phi[\rho_{QM}](\mathbf{r}_i)q_i \quad (7)$$

$\Phi[\rho_{QM}](\mathbf{r}_i)$ is the electrostatic potential due to the QM density of charge at the ith FQ placed at $\mathbf{r}_i$. Such potential can be decomposed into two contributions, one (V^N) due to the nuclei, which, in the framework of the Born−Oppenheimer approximation, remains unchanged during the solution of the electronic problem, and one (V^e) due to the electronic density:

$$\Phi[\rho_{QM}](\mathbf{r}_i) \overset{\text{def}}{=} V_i(\mathbf{P}) = V_i^N(\mathbf{P}) + V_i^e(\mathbf{P}) = \sum_{\zeta=1}^{N_n}\frac{Z_\zeta}{|\mathbf{r}_i - \mathbf{R}_\zeta|} - \int_{\mathbb{R}^3} d\mathbf{r}\,\frac{\rho^{el}(\mathbf{r})}{|\mathbf{r}_i - \mathbf{r}|}$$

where the ζ-labeled sum runs over the N_n QM nuclei, whose position we call $\mathbf{R}_\zeta$.

If one expands the electronic density $\rho^{el}(\mathbf{r})$ in an atomic basis set $\{\chi_\mu\}$, the second term of the electrostatic potential becomes:

$$V_i^e(\mathbf{P}) = -\sum_{\mu\nu} P_{\mu\nu}\int_{\mathbb{R}^3} d\mathbf{r}\,\frac{\chi_\mu(\mathbf{r})\chi_\nu(\mathbf{r})}{|\mathbf{r}_i - \mathbf{r}|} = \sum_{\mu\nu} P_{\mu\nu}V_{\mu\nu,i} \quad (8)$$

where we have introduced the "uncontracted" potential $\mathbf{V}_{\mu\nu}$ and the double sum runs on the atomic basis set. Finally, the global QM/MM energy functional for a SCF-like description of the QM portion, is

$$\mathcal{E}[\mathbf{P}, \mathbf{q}, \lambda] = \mathrm{tr}\,\mathbf{h}\mathbf{P} + \frac{1}{2}\mathrm{tr}\,\mathbf{P}\mathbf{G}(\mathbf{P}) + \mathbf{q}^\dagger\chi + \frac{1}{2}\mathbf{q}^\dagger\mathbf{J}\mathbf{q} + \lambda^\dagger\mathbf{q} + \mathbf{q}^\dagger\mathbf{V}(\mathbf{P}) \quad (9)$$

where

$$h_{\mu\nu} = \langle\chi_\mu| -\frac{\nabla^2}{2} - \sum_\zeta \frac{Z_\zeta}{|\mathbf{r} - \mathbf{R}_\zeta|}|\chi_\nu\rangle$$

and

$$G_{\mu\nu} = \sum_{\sigma\tau} P_{\sigma\tau}(\langle\mu\sigma|\nu\tau\rangle - c_x\langle\mu\sigma|\tau\nu\rangle) + c_l\langle\chi_\mu|v^{xc}|\chi_\nu\rangle$$

are the usual one- and two-electron matrices. The coefficients c_x and c_l define whether we are considering Hartree−Fock theory ($c_x = 1$, $c_l = 0$), pure DFT ($c_x = 0$, $c_l = 1$), or hybrid DFT. For the sake of brevity, we will refer to both the HF and KS matrices as Fock matrix.

We can now derive the coupled equations for the SCF procedure, i.e., the effective Fock operator and the related FQ equations. The Fock matrix is defined as the derivative of the energy with respect to the density matrix:

$$\tilde{F}_{\mu\nu} = \frac{\partial\mathcal{E}}{P_{\mu\nu}} = h_{\mu\nu} + G_{\mu\nu}(\mathbf{P}) + \mathbf{q}^\dagger\mathbf{V}_{\mu\nu} \quad (10)$$

where the effective Fock operator takes into account the interaction of the electron density with the FQs through the coupling term $\mathbf{q}^\dagger\mathbf{V}_{\mu\nu}$.

The FQs are obtained by imposing the stationarity of the global functional with respect to the charges and the Lagrangian multipliers; notice that, with respect to eq 5, a new source term arises:

$$\mathbf{D}\mathbf{q}_\lambda = -\mathbf{C}_Q - \mathbf{V}(\mathbf{P}) \quad (11)$$

Such a term, representing the coupling of the FQs with the SCF density, permits one to determine the FQs given the density matrix: it has hence the same structure of the mean-field $\mathbf{G}$ matrix and depends on the solution of the SCF equations themselves. The introduction of this nonlinear term does not represent a problem from a computational point of view, for the SCF procedure is already iterative: neither macroscopic modifications of the procedure nor an increase in the computational cost originates from the coupling with the

dx.doi.org/10.1021/ct3005062 | J. Chem. Theory Comput. XXXX, XXX, XXX−XXX

polarizable force field. The modified, iterative algorithm for the solution of the coupled SCF/FQ equations can be schematized as follows:

1. Start from a density matrix $\mathbf{P}^{(i)}$
2. Calculate the electrostatic potential $\mathbf{V}(\mathbf{P}^{(i)})$ and solve for the charges:

$$\mathbf{q}^{(i)} = -\mathbf{D}^{-1}[\mathbf{V}(\mathbf{P}^{(i)}) + \chi]$$

Notice that, as the $\mathbf{D}$ matrix does not depend on the SCF density but only on the MM atoms positions, one can invert it at the first step of the SCF procedure, keep it in memory, or store it on a disk and use it again at each step. This means that the computational cost is $O(N_q^3)$ at the first step and limited to a single matrix-vector multiplication for the other ones. Therefore, the procedure is feasible for several thousand MM atoms, since the matrix size is determined by the number of MM atoms plus the number of constraints.

3. Assemble the effective Fock matrix:

$$\tilde{F}_{\mu\nu}^{(i)} = h_{\mu\nu} + G_{\mu\nu}(\mathbf{P}^{(i)}) + \mathbf{V}_{\mu\nu}^{\dagger}\mathbf{q}^{(i)}$$

4. Solve Roothan equations and build a new density matrix:

$$\tilde{\mathbf{F}}^{(i)}\mathbf{C}^{(i+1)} = \mathbf{S}\mathbf{C}^{(i+1)}\tilde{\boldsymbol{\varepsilon}}^{(i+1)}$$

$$\mathbf{P}^{(i+1)} = \mathbf{C}^{(i+1)\dagger}\mathbf{C}^{(i+1)}$$

5. Iterate until convergence is reached.

The modified Roothan algorithm is trivially adaptable to convergence acceleration methods such as Pulay's direct inversion in the iterative subspace (DIIS).[66−68]

We are here assuming that the solute and the solvent are not covalently bonded: this limitation may be easily overcome for example by means of the so-called ONIOM[69,70] scheme, where link atoms are employed to treat the bonds between the QM and MM portions. Notice that the analytical QM/MM scheme is trivially recovered[70] once the nonadditive contributions to the low-level energy in the ONIOM scheme are neglected, and no covalent bond is present.

2.1. Coupling with the Polarizable Continuum Model.

In order to treat long-range electrostatic interactions, the FQ model has been coupled with the conductor-like version of the polarizable continuum model (C-PCM).[71−74] Such a model represents the environment by means of a conductor that surrounds a molecule-shaped cavity, which accommodates the solute and models the interaction by means of classical electrostatics. Let Ω be such a cavity, and let $\Gamma = \partial\Omega$ be the surface enclosing the cavity itself: the electrostatics equation with metallic boundary conditions reads

$$-\nabla^2 V = 4\pi\rho_M \text{ in } \Omega$$

$$V = 0 \text{ on } \Gamma \tag{12}$$

where ρ_M is the solute charge density, which we assume to be supported inside the cavity. If one decomposes the potential as the sum of the electrostatic potential produced by the solute in vacuo (Φ_M) and a reaction term (W) due to the polarization of the conductor, the Poisson equation can be solved for the reaction potential

$$-\nabla^2 W = 0 \text{ in } \Omega$$

$$W = -\Phi \text{ on } \Gamma \tag{13}$$

It is possible to recast the C-PCM problem as an integral equation[75] by introducing an apparent surface charge (ASC) σ, which represents the polarization of the conductor. Such an equation reads

$$(\mathcal{S}\sigma)(\mathbf{s}) = \int_\Gamma \frac{\sigma(\mathbf{s}')}{|\mathbf{s}-\mathbf{s}'|}\,\mathrm{d}\mathbf{s}' = -\Phi(\mathbf{s}),\ \mathbf{s}\in\Gamma \tag{14}$$

To take into account the dielectric nature of the chemical environment, the solution is scaled by a constant factor $f(\varepsilon)$ which depends on the solvent dielectric constant.[71−73] Equation 14 is solved introducing a discretization of the surface Γ in N_σ surface elements; at the center of each is placed a point charge σ_i that represents the ASC. The $\mathcal{S}$ operator is discretized as follows:[13,71,72,76]

$$\mathbf{S}_{ij} = \frac{1}{|\mathbf{s}_i - \mathbf{s}_j|}(i \neq j)$$

$$\mathbf{S}_{ii} = 1.0694\sqrt{\frac{4\pi}{a_i}}\,(i = j) \tag{15}$$

where $\mathbf{s}_i$ is the center of the ith surface element, and the molecular electrostatic potential is calculated at each discretization point. The PCM charges and the molecular potential are collected in the vectors $\boldsymbol{\sigma}$ and $\mathbf{V}$; including also the scaling factor, the discretized C-PCM equation finally reads

$$\frac{1}{f(\varepsilon)}\mathbf{S}\boldsymbol{\sigma} = -\mathbf{V} \tag{16}$$

Notice that a more sophisticated discretization technique has been presented by Scalmani and Frisch in a recent paper,[77] which implies a different definition of the discretized $\mathcal{S}$ operator.

It is possible to recast the C-PCM as a variational problem[64,65] by introducing the energy functional

$$\mathcal{E}(\boldsymbol{\sigma}) = \frac{1}{2f(\varepsilon)}\boldsymbol{\sigma}^{\dagger}\mathbf{S}\boldsymbol{\sigma} + \boldsymbol{\sigma}^{\dagger}\mathbf{V} \tag{17}$$

The (unique) minimum of eq 17 is in correspondence of the solution to eq 16, and the minimum value of the functional is the polarization energy. Notice that such a functional consists of a bilinear self-interaction term, which depends only on the ASC, and a linear term which represents the interaction of the ASC with the solute charge density: such a term depends on the model used to describe the solute. In particular, for a molecular system described with the FQ model embedded in a polarizable continuum,[26] the variational energy functional reads

$$F(\mathbf{q},\boldsymbol{\lambda},\boldsymbol{\sigma}) = \mathbf{q}^{\dagger}\chi + \frac{1}{2}\mathbf{q}^{\dagger}\mathbf{J}\mathbf{q} + \boldsymbol{\lambda}^{\dagger}\mathbf{q} + \frac{1}{2f(\varepsilon)}\boldsymbol{\sigma}^{\dagger}\mathbf{S}\boldsymbol{\sigma} + \boldsymbol{\sigma}^{\dagger}\boldsymbol{\Omega}\mathbf{q} \tag{18}$$

where

$$\sum_{i=1}^{N_q}\Omega_{ki}q_i = \sum_{i=1}^{N_q}\frac{q_i}{|\mathbf{s}_k - \mathbf{r}_i|} = V_k[\mathbf{q}]$$

is the electrostatic potential produced by the FQs at the cavity point $\mathbf{s}_k$. Notice that the interaction energy can be viewed equivalently as the interaction of the ASC with the FQs potential or the one of the FQs with the reaction potential, i.e.

dx.doi.org/10.1021/ct3005062 | J. Chem. Theory Comput. XXXX, XXX, XXX−XXX

$$\boldsymbol{\sigma}^{\dagger}\mathbf{V} = \boldsymbol{\sigma}^{\dagger}\boldsymbol{\Omega}\mathbf{q} = \mathbf{q}\boldsymbol{\Omega}^{\dagger}\boldsymbol{\sigma}$$

The coupled equations are obtained imposing the stationarity of eq 18 with respect to all its degrees of freedom. To ease the notation, we will assume that the FQ-described solute is composed by just one molecule (and hence only one constraint is present), whose total charge is Q:

$$\frac{\partial F}{\partial \mathbf{q}_i} = \sum_{j=1}^{N_q} J_{ij} q_j + \sum_{k=1}^{N_\sigma} \Omega_{ik}\sigma_k + \lambda + \chi_i = 0$$

$$\frac{\partial F}{\partial \lambda} = \sum_{i=1}^{N_q} q_i - Q = 0$$

$$\frac{\partial F}{\partial \sigma_k} = \frac{1}{f(\varepsilon)} \sum_{l=1}^{N_\sigma} S_{kl}\sigma_l + \sum_{i=1}^{N_q} \Omega_{ki} q_i = 0$$

In compact notation, introducing the $\mathbf{D}$ matrix already presented at the beginning, the coupled equations read

$$\begin{pmatrix} \mathbf{D} & \boldsymbol{\Omega}^{\dagger} \\ \boldsymbol{\Omega} & S/f(\varepsilon) \end{pmatrix} \begin{pmatrix} \mathbf{q}_\lambda \\ \boldsymbol{\sigma} \end{pmatrix} = \begin{pmatrix} -\mathbf{C} \\ 0 \end{pmatrix} \tag{19}$$

Notice that no PCM contribution appears at the right-hand side, which is consistent with the PCM having no independent source: if the FQs vanish, no polarization ASC can be produced. The coupling between the unknown charges is hence completely defined by the $\boldsymbol{\Omega}$ matrix.

In order to obtain a global, fully polarizable QM/classical energy functional, it is necessary to further couple the PCM charges and the QM density. Assuming once again the interaction to be classical:

$$E_{\mathrm{QM/PCM}} = \sum_{k=1}^{N_\sigma} \Phi[\rho_{\mathrm{QM}}](s_k)\sigma_k \tag{20}$$

In conclusion, the QM/MM/PCM functional reads

$$\begin{aligned} \varepsilon[\mathbf{P}, \mathbf{q}, \lambda, \boldsymbol{\sigma}] = {} & \mathrm{tr}\,\mathbf{hP} + \frac{1}{2}\mathrm{tr}\,\mathbf{PG}(\mathbf{P}) + \mathbf{q}^{\dagger}\boldsymbol{\chi} + \frac{1}{2}\mathbf{q}^{\dagger}\mathbf{J}\mathbf{q} \\ & + \lambda^{\dagger}\mathbf{q} + \mathbf{q}^{\dagger}\mathbf{V}_{\mathrm{FQ}}(\mathbf{P}) + \frac{1}{2f(\varepsilon)}\boldsymbol{\sigma}^{\dagger}\mathbf{S}\boldsymbol{\sigma} \\ & + \boldsymbol{\sigma}^{\dagger}\mathbf{V}_{\mathrm{PCM}}(\mathbf{P}) + \boldsymbol{\sigma}^{\dagger}\boldsymbol{\Omega}\mathbf{q} \end{aligned} \tag{21}$$

where with $\mathbf{V}_{\mathrm{FQ}}$ and $\mathbf{V}_{\mathrm{PCM}}$ we denote the QM solute's potential calculated at the MM atoms and at the PCM discretization points respectively. We notice that, from a formal point of view, the inclusion of the PCM only alters the dimensionality of the linear system: in order to include a PCM layer in the QM/MM model, the FQ $\mathbf{D}$ matrix is only to be replaced by the one defined in eq 19, and the interaction potential with the QM portion is to be calculated at both the FQs and the PCM cavity points. The same modified SCF procedure can be employed to solve the coupled equations, where the effective Fock matrix now reads

$$\tilde{F}_{\mu\nu} = h_{\mu\nu} + G_{\mu\nu}(\mathbf{P}) + \mathbf{q}^{\dagger}\mathbf{V}_{\mu\nu,\mathrm{FQ}} + \boldsymbol{\sigma}^{\dagger}\mathbf{V}_{\mu\nu,\mathrm{PCM}}$$

where again the uncontracted potential has to be calculated both at the MM atoms ($\mathbf{V}_{\mu\nu,\mathrm{FQ}}$) and at the PCM cavity points ($\mathbf{V}_{\mu\nu,\mathrm{PCM}}$). Finally, the FQs and the PCM charges are calculated at the same time solving eq 19.

$$\begin{pmatrix} \mathbf{D} & \boldsymbol{\Omega}^{\dagger} \\ \boldsymbol{\Omega} & S/f(\varepsilon) \end{pmatrix} \begin{pmatrix} \mathbf{q}_\lambda \\ \mathbf{s} \end{pmatrix} = -\begin{pmatrix} \mathbf{C} \\ 0 \end{pmatrix} - \begin{pmatrix} \mathbf{V}_{\mathrm{FQ}} & (\mathbf{P}) \\ \mathbf{V}_{\mathrm{PCM}} & (\mathbf{P}) \end{pmatrix} \tag{22}$$

As the account of PCM does not modify the theoretical framework but simply makes the notation more cumbersome, in the following we will only deal with the QM/FQ contributions.

Before discussing linear response theory for a QM/FQ(/PCM) model, it is worth saying a few words comparing our model to other polarizable QM/MM approaches. While there exist previous implementations of an equivalent model,[32−36] we will focus in particular on the one developed by Curutchet et al.[9] and extended by Steindal et al,[20] the latter also including the PCM embedding. We will refer to such a method as MMpol. In this model, the polarizability of the MM layer is introduced by means of Thole's point dipole method,[24] where all the atoms are endowed with a (nonpolarizable) point charge and a polarizability, which gives rise to an induced dipole moment. Without going into the technical aspects of the strategy, the interaction between the various layers can be grouped into two different contributions: an electrostatic (es) one and a polarization (pol) one, which describe the interaction of the QM density (or PCM ASC) with the charges and induced dipoles, respectively:

$$E_{\mathrm{es}} = \sum_m q_m V(\mathbf{r}_m),\ E_{\mathrm{pol}} = -\sum_a \boldsymbol{\mu}_a^{\mathrm{ind}}\mathbf{F}_a$$

where $\mathbf{F}$ is the electric field produced by the interacting density of charge, the m index runs over the charge sites, and the a index runs over the dipole sites. The MM energy is also the sum of an electrostatic contribution (i.e., the interaction energy of the MM charges) and a polarization contribution, which takes into account the interaction of the induced dipoles with the MM point charges. The induced dipoles can be obtained by solving a matrix equation

$$\mathbf{K}\boldsymbol{\mu} = -\mathbf{F}$$

where the diagonal blocks of the $\mathbf{K}$ matrix are the polarizabilities of each site and the $i-j$ off-diagonal block is the dipole−dipole interaction tensor between sites i and j. If the PCM is included in the description, similar equations are obtained: the dimensionality of the problem, on the other hand, is increased by the number of PCM discretization points.[20] The most apparent difference between the aforementioned methods and the one we are proposing here is the method of including the polarization in the MM layer. While it is possible to relate the atomic hardnesses and the molecular polarizability,[25] the two approaches differ in several features. First, the atomic parameters in the FQ model are scalars: this is due to the fact that a fluctuating charge is a zeroth order multipole, which is isotropic by nature. This implies that polarization effects in a planar molecule cannot have out-of-plane contributions whenever the FQs are placed at atomic sites. This is not the case of the MMpol, as the induced dipoles are instead vector quantities. Notice that the FQ model can easily recover out-of-plane effects by considering additional polarization sites,[78] which can be placed out of the molecular plane. Another significant difference is that the MMpol method distinguishes explicitly between static and polarization contributions, the first being represented by fixed point charges and the second by induced dipoles. This is perfectly consistent with what is called a *nonequilibrium*[79−82] regime in the PCM framework, where the

dx.doi.org/10.1021/ct3005062 | J. Chem. Theory Comput. XXXX, XXX, XXX−XXX

polarization contributions represent the electronic degrees of freedom of the classical portion. Such a partition is less evident in the FQ model, as both static and polarization contributions are calculated together. Nevertheless, in the FQ model, the static contribution can be seen as arising from the differences in atomic electronegativities, while the polarization contribution is due to the hardnesses, which appears in the definition of the FQ matrix **D** (see eq 5). This means that the polarization of an FQ-described molecule gives rise to a charge separation (as an example, if a water molecule is H-bonded to some acceptor molecule, the involved hydrogen atom will have a different charge than the other). Notice that such a separation is crucial in the parametrization procedure, which is less explored for the FQ model than for Thole's point dipole method.

There is also a substantial difference in the way the polarizable MM layer interacts with the QM (and PCM) one: in the MMpol model, both the electrostatic potential and the electric field are involved. In particular, the size of all the MMpol related quantities, including the **K** matrix, scales as three times the number of polarization sites. This means that with the same computational effort, the FQ model can manage an almost 3 times larger number of polarization sites, giving the model more flexibility. We have also preferred to adopt a model which only involves the electrostatic potential, because it is more formally consistent with the modern PCM implementations.[76] This can be helpful in coding not only response properties but especially analytical derivatives, which will be the subject of a forthcoming communication. Notice that, while the FQ matrix might be, in principle, smaller than the MMpol one, it is known that a potential matrix (i.e., a matrix where the interactions scale as $1/r$) is usually ill-conditioned, while a field matrix is not affected by such a problem.[73] This means that iterative procedures are more efficient in solving the MMpol equations than the FQ ones. On the other hand, matrix inversion is convenient when it is feasible, which is usually the case for our QM/FQ(/PCM) method, especially if a large enough number of MM molecules is included such that a regular PCM cavity can be employed. A formal difference between our approach and MMpol is, finally, that we have started our derivation from a global, variational functional of all the polarizable degrees of freedom, both quantum mechanical and classical. From a formal point of view, such a formulation makes it easier to obtain the coupled equations and is a convenient starting point to formulating analytical derivatives of the energy. In the practice, simultaneous optimization strategies, where both the quantum and classical densities are optimized at the same time, can be explored.[65] The latter have been shown to be advantageous when the computational effort to treat the classical portion is larger than the one required to solve the QM problem.

3. LINEAR RESPONSE THEORY

Let $\tilde{\mathcal{F}}$ be the FQ/Fock operator defined in eq 10. According to Frenkel's principle, the time evolution of a system described by a single-determinant wave function $|\Phi\rangle$ has to satisfy the least action principle with orthogonality constraints. For the QM/FQ system, the action will be the sum of the QM action and an interaction term, contained in the FQ/Fock operator:

$$\mathcal{S} = \langle \Phi | i\partial_t - \mathcal{H}_{\text{eff}} | \Phi \rangle = \sum_{i=1}^{N} \langle \varphi_i | i\partial_t - \tilde{\mathcal{F}} | \varphi_i \rangle$$

where the sum runs over the N occupied canonical spinorbitals. As usual, occupied orbitals are labeled as i, j, ...; virtual orbitals as a, b, ...; and generic orbitals as p, q, ... The Frenkel equations read

$$\langle \delta\varphi_i | i\partial_t - \tilde{\mathcal{F}} | \varphi_i \rangle = 0,\ \langle \delta\varphi_i | \varphi_j \rangle = 0\ \forall\ i, j \tag{23}$$

Here, only the "bra" variation is considered; the "ket" term results in the complex conjugate equation, which we will just recover at the end of the derivation. First order perturbation theory can be used to make eq 23 treatable. By expanding the molecular orbitals to the first order

$$|\varphi_i(t)\rangle = |\varphi_i^{(0)}(t)\rangle + \lambda |\varphi_i^{(1)}(t)\rangle$$

one can write a zeroth order and a first order equation from eq 23.

The QM/FQ coupling potential depends on the FQs, which solve eq 11 and in turn depend on the molecular potential, which depends on the orbitals. The generic matrix element of such a coupling will be

$$\mathbf{q}^\dagger \mathbf{V}_{pq} = \mathbf{V}_{pq}^\dagger \mathbf{q} = \sum_{k=1}^{N_q} q_k[\varphi] \langle \varphi_p | \frac{1}{|\mathbf{r} - \mathbf{r}_k|} | \varphi_q \rangle \tag{24}$$

In the perturbative expansion, the expansion of the $\hat{G}$ and $\mathbf{q}^\dagger\hat{\mathbf{V}}$ operators has to be carried out. The zeroth order equation corresponds to the unperturbed equation

$$\begin{aligned} &(\hat{h} + \hat{G}^{(0)} + \hat{\mathbf{V}}^\dagger \mathbf{q}^{(0)}) |\varphi_i^{(0)}(t)\rangle \\ &\quad = \tilde{\mathcal{F}}^{(0)} |\varphi_i^{(0)}(t)\rangle \\ &\quad = i\frac{\partial}{\partial t} |\varphi_i^{(0)}(t)\rangle \end{aligned} \tag{25}$$

whose solution is

$$|\varphi_i(t)^{(0)}\rangle = |\phi_i\rangle e^{-i\varepsilon_i t},\ \tilde{\mathcal{F}} |\phi_i\rangle = \varepsilon_i |\phi_i\rangle$$

that is, one recovers the time-independent framework, as expected.

The first order equation is obtained by collecting all the terms which depend linearly on λ:

$$\begin{aligned} &\tilde{\mathcal{F}}^{(0)} |\varphi_i^{(1)}(t)\rangle + (\hat{G}^{(1)}(t) + \hat{\mathbf{V}}^\dagger \mathbf{q}^{(1)}(t)) |\varphi_i^{(0)}(t)\rangle \\ &\quad = i\frac{\partial}{\partial t} |\varphi_i^{(1)}(t)\rangle \end{aligned} \tag{26}$$

Because of orthogonality constraints, the first order contribution to the molecular orbitals only projects on the virtual orbitals space, i.e.:

$$|\varphi_i^{(1)}(t)\rangle = \sum_a P_{ia}(t) |\phi_a\rangle e^{-i\varepsilon_i t} \tag{27}$$

The first term on the right-hand-side can be simplified:

$$\begin{aligned} \tilde{\mathcal{F}}^{(0)} |\varphi_i^{(1)}(t)\rangle &= \tilde{\mathcal{F}}^{(0)} \sum_a P_{ia}(t) |\phi_a\rangle e^{-i\varepsilon_i t} \\ &= \sum_a \varepsilon_a P_{ia}(t) |\phi_a\rangle e^{-i\varepsilon_i t} \end{aligned}$$

The time derivative (which will be indicated with a dot for brevity) gives two different contributions:

$$i\frac{\partial}{\partial t}|\varphi_i^{(1)}(t)\rangle = \varepsilon_i \sum_a P_{ia}(t)|\phi_a\rangle e^{-i\varepsilon_i t} + i\sum_a \dot{P}_{ia}(t)|\phi_a\rangle e^{-i\varepsilon_i t}$$

By substituting in the first equation of eq 26, one gets

$$\sum_a (\varepsilon_a - \varepsilon_i)P_{ia}(t)|\phi_a\rangle e^{-i\varepsilon_i t} + (\hat{G}^{(1)}(t) + \hat{\mathbf{V}}^\dagger \mathbf{q}^{(1)}(t))|\phi_i\rangle e^{-i\varepsilon_i t} = i\sum_a \dot{P}_{ia}(t)|\phi_a\rangle e^{-i\varepsilon_i t} \tag{28}$$

and by projecting on $\langle\varphi_a|$ and eliminating the phase factor:

$$(\varepsilon_a - \varepsilon_i)P_{ia}(t) + \langle\phi_a|\hat{G}^{(1)}(t) + \hat{\mathbf{V}}^\dagger \mathbf{q}^{(1)}(t)|\phi_i\rangle = i\dot{P}_{ia}(t) \tag{29}$$

It is a well-known result that

$$\langle\phi_a|G^{(1)}(t)|\phi_i\rangle = \sum_{jb} P_{jb}(t)\langle aj\,||\,ib\rangle + P_{jb}^*(t)\langle ab\,||\,ij\rangle \tag{30}$$

where

$$\langle pq||rs\rangle = \langle pq|rs\rangle - \langle pq|sr\rangle$$

are standard antisymmetrized bielectronic integrals. Moving to the coupling potential:

$$\mathbf{V}_{ai}^\dagger \mathbf{q}^{(1)} = \langle\phi_a|\hat{\mathbf{V}}^\dagger \mathbf{q}^{(1)}(t)|\phi_i\rangle = \sum_{k=1}^{N_q} \langle\phi_a|\frac{q_k^{(1)}}{|\mathbf{r} - \mathbf{R}_k|}|\phi_i\rangle \tag{31}$$

To calculate $\mathbf{q}^{(1)}$, the perturbed FQ equations need to be solved:

$$\mathbf{D}\mathbf{q}^{(1)} = -(\mathbf{C}_Q + \mathbf{V}(\varphi))^{(1)}$$

where the constant term $\mathbf{C}_q$ does not give rise to any contribution. The perturbed molecular potential can be derived from its definition, by inserting the perturbative expansion of the molecular orbitals

$$V_k = \int_{\mathbb{R}^3} \mathrm{d}r \frac{\sum_{i=1}^N (\varphi_i^{(0)}(t) + \varphi_i^{(1)}(t))^*(\varphi_i^{(0)}(t) + \varphi_i^{(1)}(t))}{|\mathbf{r} - \mathbf{R}_k|} = V_k^{(0)} + V_k^{(1)}$$

where we have dropped higher order terms and

$$V_k^{(1)} = \int_{\mathbb{R}^3} \mathrm{d}\mathbf{r} \sum_i \frac{\varphi_i^{(0)*}(t)\varphi_i^{(1)}(t) + \varphi_i^{(1)*}(t)\varphi_i^{(0)}(t)}{|\mathbf{r} - \mathbf{R}_k|} \tag{32}$$

Substitution of eq 27 into eq 32 yields

$$V_k^{(1)} = \sum_{ia} P_{ia}(t)\langle\phi_i|\frac{1}{|\mathbf{r} - \mathbf{R}_k|}|\phi_a\rangle + P_{ia}^*(t)\langle\phi_a|\frac{1}{|\mathbf{r} - \mathbf{R}_k|}|\phi_i\rangle \tag{33}$$

Hence, the perturbed FQ equations have the following solution:

$$\mathbf{q}_k^{(1)} = -\mathbf{D}^{-1}[\sum_{ia} P_{ia}(t)\mathbf{V}_{ia} + P_{ia}^*(t)\mathbf{V}_{ai}] \tag{34}$$

Whenever the orbitals are real, $\mathbf{V}_{ai} = \mathbf{V}_{ia}$. By exploiting Casida et al.'s notation,[83] the following matrices are defined:

$$\tilde{A}_{ai,bj} = (\varepsilon_a - \varepsilon_i)\delta_{ab}\delta_{ij} + \langle aj\,||\,ib\rangle - \sum_{kl}^{N_q} \mathbf{V}_{ia}^\dagger \mathbf{D}^{-1}\mathbf{V}_{jb} \tag{35}$$

$$\tilde{B}_{ai,bj} = \langle ab\,||\,ij\rangle - \sum_{kl}^{N_q} \mathbf{V}_{ia}\mathbf{D}^{-1}\mathbf{V}_{bj} \tag{36}$$

Therefore, eq 29 becomes:

$$\sum_{bj} \tilde{A}_{ai,bj}P_{jb}(t) + \tilde{B}_{ai,bj}P_{jb}^*(t) = i\dot{P}_{ia}(t) \tag{37}$$

or, in the frequency domain:

$$\sum_{bj} \tilde{A}_{ai,bj}P_{jb}(\omega) + \tilde{B}_{ai,bj}P_{jb}^*(-\omega) = \omega\dot{P}_{ia}(\omega) \tag{38}$$

If we put

$$\mathbf{X} = \mathbf{P}(\omega),\ \mathbf{Y} = \mathbf{P}^*(-\omega)$$

and take the complex conjugate of eq 37, we finally get the so-called Casida's equations[83] for the FQ/QM linear response theory:

$$\begin{pmatrix} \tilde{\mathbf{A}} & \tilde{\mathbf{B}} \\ \tilde{\mathbf{A}}^* & \tilde{\mathbf{B}}^* \end{pmatrix}\begin{pmatrix} \mathbf{X} \\ \mathbf{Y} \end{pmatrix} = \omega\begin{pmatrix} 1 & 0 \\ 0 & -1 \end{pmatrix}\begin{pmatrix} \mathbf{X} \\ \mathbf{Y} \end{pmatrix} \tag{39}$$

As stated before, a generalization to the full QM/MM/PCM scheme is easily obtained by substituting through the derivation the FQs vectors with the FQ + PCM ones and the **D** matrix with the one defined in eq 19. In particular, the modified response equations will include two contributions arising from the perturbed FQs ($\mathbf{V}_{\mathrm{at,FQ}}^\dagger \mathbf{q}^{(1)}$) and PCM charges ($\mathbf{V}_{\mathrm{at,FQ}}^\dagger \mathbf{s}^{(1)}$), where, again, the interaction potential will be calculated at the FQs and at the PCM cavity discretization points, respectively. For the perturbed FQ and PCM charges, one obtains similarly a perturbed FQ/PCM equation:

$$\begin{pmatrix} \mathbf{D} & \mathbf{\Omega}^\dagger \\ \mathbf{\Omega} & S/f(\varepsilon) \end{pmatrix}\begin{pmatrix} \mathbf{q}_\lambda^{(1)} \\ \boldsymbol{\sigma}^{(1)} \end{pmatrix} = -\begin{pmatrix} \mathbf{V}_{\mathrm{FQ}}^{(1)} \\ \mathbf{V}_{\mathrm{PCM}}^{(1)} \end{pmatrix} \tag{40}$$

where the perturbed potential is defined as in eq 33.

Notice finally that, if we take the zero frequency limit of the response equations, the static coupled-perturbed Hartree−Fock (CPHF) equations are obtained.

4. NUMERICAL RESULTS

In this section, we will present some preliminary numerical results to show the potentialities of our model. First, we discuss the convergence of the results with respect to the number of explicit solvent molecules and how it is affected by the presence of the polarizable continuum. Using a system of reduced dimensionality as a model, we will proceed to decompose and analyze the different contributions to the excitation energy given by the polarizable environment. Next, as proofs of concept, we will apply our methodology to calculate the solvatochromic shift of a molecule in solution and of a chromophore embedded in a biological matrix. We would like to stress that these last results are to be considered just examples of the potentialities of the method: a detailed study of the aforementioned systems is far beyond the scope of this article.

Let us start by discussing how the presence of a polarizable continuum affects the convergence of the properties with

dx.doi.org/10.1021/ct3005062 | J. Chem. Theory Comput. XXXX, XXX, XXX−XXX

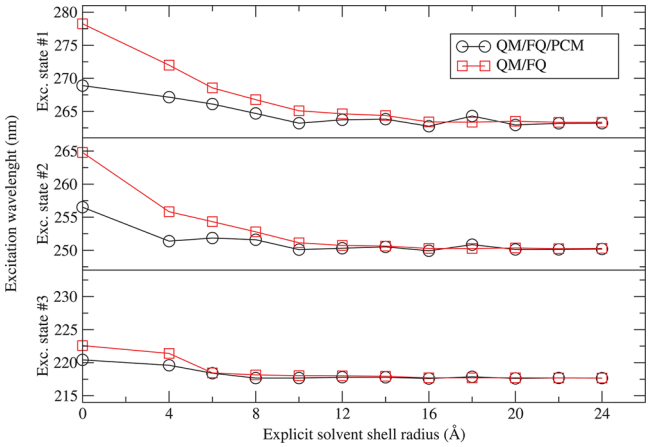

Figure 1. Electronic excitation wavelengths (nm) for the first three excited states of pyrimidine as a function of the explicit solvent cutting radius, with and without PCM.

Table 1. Converged Charges Obtained in the QM/FQ(/PCM) Simulations of the Pyrimidine +2 Water Molecules Cluster[a]

atom	QM/FQ	QM/FQ/PCM
O	−0.5587	−0.5973
H*	0.3370	0.3605
H	0.2217	0.2368

[a]The H-bonded hydrogen is labeled H*.

respect to the number of solvent molecules considered. In Figure 1, we report electronic excitation wavelengths for the first three electronic states of pyrimidine in aqueous solution obtained with and without the inclusion of the polarizable continuum embedding as a function of the cutting radius for the atomistic portion. The configurations were taken from a molecular dynamics simulation, and concentric spheres placed at the center of the pyrimidine molecule were cut and then all the water molecules whose oxygen atom was inside the sphere included in the atomistic portion. For the QM/FQ/PCM simulations, a spherical PCM cavity was employed with a radius 1.5 Å larger than the one of the cut sphere. Time dependent (TD) DFT was employed to obtain the transition energies, using the long-range corrected CAM-B3LYP[84] exchange-correlation functional and the aug-N07D[85,86] basis set. The parameters for the FQ force field were taken from Rick et al.[25] $R = 0$ in Figure 1 corresponds to the calculation without the inclusion of explicit solvent molecules, i.e., *in vacuo* or with a standard PCM approach with a molecule shaped cavity, respectively. From our results, it comes out that the use of PCM to account for long-range interactions permits one to limit the number of solvent molecules to be included in the cluster to reach a given accuracy; in fact, the calculations are at convergence with a cutting radius of 8−10 Å. Moreover, the combined FQ/PCM approach does not require a molecule-shaped cavity: this is greatly advantageous in terms of computational cost, as the number of points required to obtain a good numerical representation of the PCM ASC when the cavity is (highly) regular is much smaller than what is required for standard (irregular) cavities.[77]

When a QM/FQ(/PCM) model is used to calculate vertical excitation energies of a molecule in the framework of linear response theory, two different contributions arise: a polarization contribution and a response one. The former is due to the interaction of the polarizable embedding with the electronic density: such an effect is introduced in the SCF calculation as a consequence of the coupling defined in eq 7, which is responsible for the FQ contribution to the Fock operator defined in eq 10. This is not a prerogative of polarizable embeddings and can be treated by means of suitably tailored fixed charges in the electrostatic embedding approach. The latter effect is due to the FQ contribution to the molecular response; as summarized in eqs 35 and 36, it is present only when a polarizable force field is employed. The polarization contribution is expected to be by far the leading one, as it can produce a major rearrangement in the charge density of the QM-described molecule. Continuum solvation literature[80] offers a powerful interpretative tool to explain the different weight of the two distinct corrections to the excitation energy, i.e., the concept of *non-equilibrium*. When the environment is described by a classical charge density, it is in fact mandatory to consider the time scale of the phenomena under study. A "static" phenomenon, such as the solvation of a molecule in its ground state, is an *equilibrium* situation, i.e., the polarizable continuum is fully polarized according to the laws of electrostatics. When a fast phenomenon, such as an electronic transition, occurs, it is unphysical to consider the continuum to be fully polarized and instantaneously equilibrated with the electronic density of the excited state.[81] Only the fast (i.e., electronic) degrees of freedom of the environment relax, whereas the other degrees of freedom do not, therefore giving rise to a nonequilibrium system.[79] From a more quantitative point of view, if one models the solvent in terms of its dielectric constant, equilibrium phenomena are described in terms of its *static* dielectric constant, whereas nonequilibrium ones are described in terms of the optical one. As this latter is usually much smaller than the static one (as an example, for water ε = 78.3553 and ε_∞ = 1.7778), the response effect, which depends on the optical permittivity, is smaller as well.

As already mentioned, the QM/FQ(/PCM) picture is consistent with a nonequilibrium regime, as the response

Table 2. Vertical Absorption Energies (eV) and Oscillator Strengths for the First Five Excited States of Pyrimidine in Vacuo and Solvatochromic Shifts As Obtained with a Fixed-Charge (QM/MM) and Fluctuating Charge (QM/FQ) Approach, Including the PCM Embedding (/PCM) for the Last Columns

	vacuum		QM/MM		QM/FQ		QM/MM/PCM		QM/FQ/PCM	
state	ε	f	$\Delta\varepsilon$	Δf	$\Delta\varepsilon$	Δf	$\Delta\varepsilon$	Δf	$\Delta\varepsilon$	Δf
B1 $n \leftarrow \pi^*$	4.483	0.0053	0.308	0.0002	0.309	0.0003	0.400	0.0063	0.403	0.0071
A2 $n \leftarrow \pi^*$	4.862	0.0000	0.293	0.0000	0.295	0.0000	0.406	0.0000	0.408	0.0000
B2 $\pi \leftarrow \pi^*$	5.808	0.0438	0.011	0.0043	0.008	0.0071	−0.067	0.0426	−0.042	0.0438
A2 $n \leftarrow \pi^*$	5.955	0.0000	0.245	0.0000	0.246	0.0000	0.292	0.0000	0.295	0.0000
B1 $n \leftarrow \pi^*$	6.284	0.0055	0.231	0.0005	0.230	0.0005	0.289	0.0016	0.295	0.0026

dx.doi.org/10.1021/ct3005062 | J. Chem. Theory Comput. XXXX, XXX, XXX−XXX

Table 3. Vertical Absorption Energies (eV) and Oscillator Strengths for the First Five Excited States of Pyrimidine in Vacuo and Solvatochromic Shifts As Obtained with a Full QM Approach, Including the PCM Embedding (/PCM) for the Last Columns[a]

	vacuum		QM		QM/PCM			
state	ε	f	$\Delta\varepsilon$	Δf	$\Delta\varepsilon$	Δf	QM/FQ/PCM	
B1 $n \leftarrow \pi^*$	4.483	0.0053	0.324	−0.0014	0.417	0.0001	0.403	0.0071
A2 $n \leftarrow \pi^*$	4.862	0.0000	0.305	0.0000	0.426	0.0000	0.408	0.0000
B2 $\pi \leftarrow \pi^*$	5.808	0.0438	0.005	0.0097	−0.050	0.0445	−0.042	0.0438
A2 $n \leftarrow \pi^*$	5.955	0.0000	0.241	0.0000	0.296	0.0000	0.295	0.0000
B1 $n \leftarrow \pi^*$	6.284	0.0055	0.225	−0.0017	0.291	0.0007	0.295	0.0026

[a]To ease the comparison, the QM/FQ/PCM results are reported as well in the last two columns.

Table 4. Vertical Excitation Energies (eV) Obtained As an Average over 100 MD Snapshots with TIP3P (Non-Polarizable) and FQ Electrostatics for the First Three Excited States of Pyrimidine in Aqueous Solution[a]

state	QM/MM/PCM	QM/FQ/PCM
B1 $n \leftarrow \pi^*$	4.85	4.79
A2 $n \leftarrow \pi^*$	5.29	5.25
B2 $\pi \leftarrow \pi^*$	5.77	5.75

[a]The polarizable embedding is included in both models.

Table 5. Vertical Excitation Energies (eV) and Oscillator Strengths for the First Three Excited States of Pyrimidine Surrounded by 80 Molecules of Water at the QM/FQ/PCM and Full QM/PCM Levels[a]

	FQ/PCM		QM/PCM	
state	ε	f	ε	f
B1 $n \leftarrow \pi^*$	4.999	0.0079	5.002	0.0133
A2 $n \leftarrow \pi^*$	5.271	0.0003	5.283	0.0002
B2 $\pi \leftarrow \pi^*$	5.890	0.0547	5.799	0.0602

[a]The configuration is the same used to obtain the point at 8 Å in Figure 1.

contribution only depends on the **D** matrix, which in turn depends on the atomic hardnesses. Such parameters describe the response properties of the classical system[52,62] and are hence related to its electronic degrees of freedom, while the "equilibrium" contribution is contained in the electronegativities, which is consistent with other polarizable QM/MM models.[20,40] Notice that the definition of the equilibrium regime, which would be required for instance to study fluorescence, is not trivial. In a QM/MM approach, one needs to consider explicitly the relaxation of the nuclear degrees of freedom of the environment, as an example by means of a molecular dynamics simulation.

To better understand the relative importance of the static and polarization contributions, we report vertical excitation energies for the first excited states of pyrimidine in aqueous solution, including explicitly two molecules of solvent. Such a picture has been proposed and validated by Karelson and Zerner,[87,88] who have shown that such a small model can be used to accurately reproduce solvatochromic shifts of the $n \leftarrow \pi^*$ transitions. A similar model has also been used by Gao and Byun,[89] who also analyzed the different contributions to the solvatochromic shift due to a polarizable embedding. Here, we will describe the explicit solvent molecules both with the QM/FQ model and with a fixed-charge QM/MM approach, where we will employ the (converged) FQ charges from the previous simulation. This second calculation will therefore include only the "static" contribution and allow us to estimate the importance of the polarization. Such an analysis will be repeated including also the PCM embedding (the data are labeled QM/FQ/PCM and QM/MM/PCM, respectively). The geometry of the complex has been optimized at the DFT level, using the popular B3LYP[90] exchange-correlation functional and the aug-N07D[85,86] basis set. Long range solvation effects have been included in the optimization by means of the PCM. The resulting geometry is given as Supporting Information. The converged charges with and without PCM for the two water molecules are reported in Table 1. Notice how the H-bonded hydrogen has a different (larger) charge than the other one. Table 2 shows vertical absorption energies for the first five excited states in vacuo and the solvatochromic shifts obtained with the four discussed representations of the solvent, i.e., fixed charge and FQ QM/MM, with and without including the PCM embedding. The QM portion has been described with time dependent DFT (TDDFT), using the long-range corrected CAM-B3LYP[84] exchange-correlation functional and the aug-N07D basis set. As expected, the static contribution is by far the largest one, consistent with the results of Gao and Byun;[89] on the other hand, the polarization contribution seems to have a larger effect on oscillator strengths. Notice that the FQ results are greatly influenced by the fact that the charges are equilibrated with the electronic density, as it is apparent from Table 1: a nonpolarizable force field would either not discriminate between the two hydrogen atoms or require an *ad hoc* electrostatic parametrization, which is in some sense automatically included in the QM/FQ approach by the coupling of the QM and FQ equations.

In Table 3, we report the shifts obtained when treating the whole cluster at the QM level. As the cluster model has been proved to be accurate, this represents a first benchmark calculation of our QM/FQ(/PCM) model if only short-range effects are considered: despite no tailored parametrization being employed, the agreement is surprisingly good.

The small model has been shown to be able to reproduce accurately the solvatochromic shifts for $n \leftarrow \pi^*$ transitions: if a $\pi \leftarrow \pi^*$ transition is considered, a representation of the solvent where both the explicit molecules lie in the same plane as the solute becomes poorer, because the mainly involved orbitals both have a nodal plane in correspondence with the molecular plane. Moreover, the (slow) dynamics of the solvent is not yet taken into account: this can be done by means of a mixed molecular dynamics (MD)−QM/MM approach, where a MD simulation is run and absorption properties are calculated as an average over a certain number of configurations. We report in Table 4 the results of such a composite approach, where 100 MD configurations have been employed (all the details of the MD simulation can be found in ref 91). The nonpolarizable results have been obtained using the TIP3P[92] model for water. A 16.5 Å sphere, centered on the pyrimidine molecule,

dx.doi.org/10.1021/ct3005062 | J. Chem. Theory Comput. XXXX, XXX, XXX−XXX

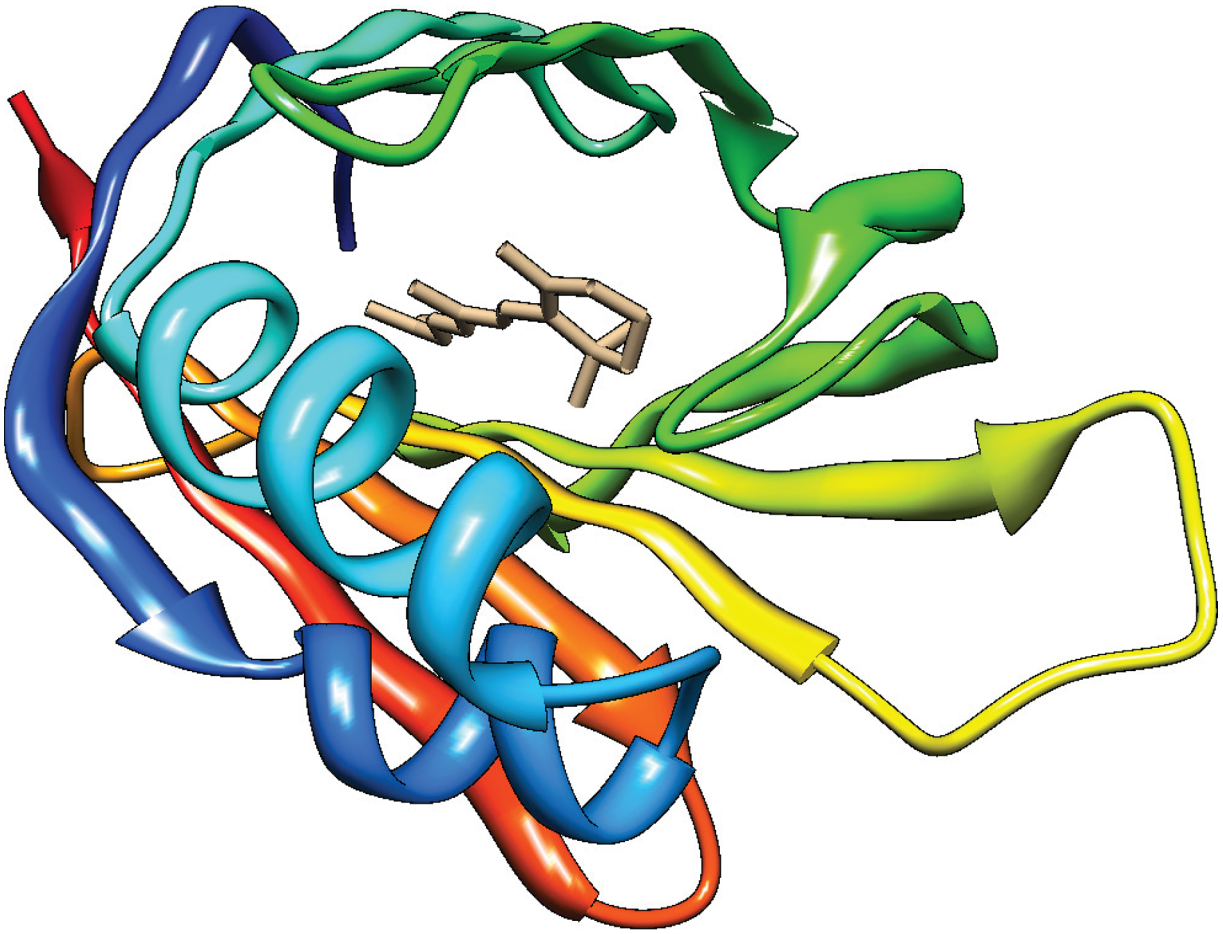

Figure 2. Retinal chromophore in a rhodopsin mimic.

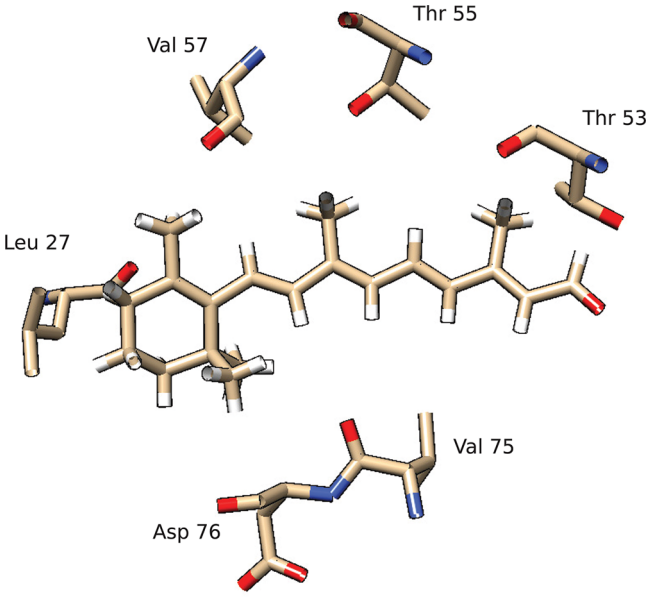

Figure 3. A closer view of the retinal chromophore.

containing approximately 485 molecules of solvent, has been cut from every MD snapshot. PCM embedding was introduced surrounding the cut sphere with an 18 Å spherical cavity; the conductor-like fashion of the model (C-PCM) has been employed. Again, the linear response calculations have been performed employing TDDFT with the CAM-B3LYP functional and the aug-N07D basis set. The results are very close to the ones obtained by Biczysko et al.[92] and with experimental data they report (4.84 eV for the first excited state, which corresponds to a solvatochromic shift of ~2600 cm^{-1}, to be compared to our result of ~2500 cm^{-1} and to the experimental value of ~2700 cm^{-1}).

Table 6. Vertical Excitation Energies (eV) of the Retinal Chromophore (First Four States) in Vacuo and in a Rhodopsin Mimic

state	vacuum	PCM	QM/MM	QM/FQ
1	3.39	3.15	3.17	3.18
2	3.59	3.82	3.95	3.83
3	4.72	4.53	4.51	4.51
4	4.87	4.83	4.78	4.74

A more quantitative comparison between the QM/FQ/PCM and a full QM description can be obtained employing a larger cluster of solvent molecules, for which the results with respect to the number of explicit molecules are already at convergence. In Table 5, we compare the results obtained for the first three excited states of a pyrimidine−water cluster corresponding to a, 8 Å cutting radius (see Figure 1) employing both the QM/FQ/PCM and a full QM/PCM approach, where both the solute and the solvent are described at the same level of theory. Because of the noticeable dimension of the system, we have employed a smaller basis set: in particular, the simulations have been performed at the CAM-B3LYP level of theory with the 6-31G* basis set. The agreement between QM/FQ/PCM and QM/

dx.doi.org/10.1021/ct3005062 | J. Chem. Theory Comput. XXXX, XXX, XXX−XXX

PCM ones is remarkable, especially for the $n \leftarrow \pi^*$ transitions. We would like to point out that a full QM treatment of the solute−solvent cluster is not only computationally very demanding but also of difficult interpretation. As it is well-known,[93] with most approximate exchange correlation functionals, a huge manifold of unphysical, low-lying charge-transfer states is introduced by the surrounding water molecules. This is the reason why we limited this analysis to the first three excited states; such a problem is of course not present when the solvent is described classically.

As a last numerical application, we report calculated data for the vertical excitation energy of the retinal chromophore in a rhodopsin mimic (see Figures 2 and 3 for a pictorial view), whose photophysics is being currently investigated by Olivucci and co-workers.[94] Again, the CAM-B3LYP functional and the aug-N07D basis set were employed. Of course, this is to be regarded just as a proof of concept: a thorough study of such a complex system is far beyond the aim of this article. Moreover, the set of parameters employed to describe the FQ polarizable electrostatics is taken from the literature[57] and has been determined to reproduce the properties of a set of small molecules: the same authors show[58] that, moving to larger molecules such as a protein, the hardnesses need to be rescaled to avoid a polarization catastrophe. Hence, a thorough work of parametrization is to be done before using our methodology to reproduce experimental properties of a complex system with good accuracy. Nevertheless, the results obtained by scaling the atomic hardness as suggested by ref 58 without any further refinement are consistent with both standard QM/MM results, where QEq[45] charges were employed, and with the ones obtained with the protein modeled as a polarizable continuum. For the latter calculation, we used the IEF-PCM[95,96] model describing the protein with a static dielectric constant of 15, which is consistent with the large number of crystallization water molecules included in the model,[97] and an optical dielectric constant of 2, as suggested in ref 40. For the QM/FQ calculation, all the residues were constrained to have a fixed charge according to the standard AMBER topology.[98] The results obtained with such a methodology are shown in Table 6. The agreement between our QM/FQ method and other, more thoroughly tested methodologies, is very good, and therefore our method, especially if coupled to a preliminary parametrization work, seems to be a very promising strategy to investigate the photophysical properties of chromophores embedded in a protein matrix.

5. CONCLUSIONS AND PERSPECTIVES

In this contribution, we have presented a fully polarizable QM/classical Hamiltonian where three different levels of theory are coupled: a quantum mechanical one, based on SCF-like methods; a classical, atomistic one, based on the fluctuating charge model; and a further classical one, based on the polarizable continuum model. The energy and the linear response equations for excited states have been derived and implemented. Some technical aspects about convergence of the results with respect to the size of the explicit, classical region have been discussed, and some preliminary results have been presented, both for solute/solvent systems and for a chromophore embedded in a protein matrix. The results obtained are always consistent with more tested methodologies, even for large systems for which a suitable, QM/MM oriented parametrization is still lacking. While we have shown that the polarization effects are small for the system analyzed if compared in magnitude with the one due to the electrostatic polarization of the ground state electronic density, the polarizable embedding offers a much more general tool, whose usage can become mandatory when one is interested in phenomena involving excited state properties. Extension of our model to analytical first and second derivatives is also very relevant in this field and will be presented in a forthcoming work by our group.

To end these final remarks, we point out that parametrization still remains a critical issue of our method, especially when one is interested in large biological systems. It is well-known that the FQ model overestimates polarization effects, and this can give rise to numerical instabilities or unphysical results. A proper definition of the atomic hardnesses in the condensed phase needs to be further investigated. A consistent, general set of parameters will permit one to fully exploit the model, starting from MD simulations[26] and ending with response property calculations using the same model and code, by means of powerful and user-friendly protocols.

APPENDIX A. SOME FORMAL CONSIDERATIONS

Let us consider eq 20 from a calculus-of-variations point of view. In the presence of a set of classically described, polarizable molecules embedded in a polarizable continuum, the (free) energy of a solute described at the SCF level of theory can be viewed as the minimum of such a functional with respect to three different densities of charge: the SCF one and the ones introduced by the FQs and the PCM, respectively. From the mathematical point of view, there is a major difference between these densities: the PCM one lives in a vector space, i.e.:

$$\boldsymbol{\sigma} \in \mathbb{R}^{N_\sigma}$$

and therefore the minimization is free. On the contrary, this is not the case for the other two densities. The only acceptable FQs are the ones satisfying the total charge constraint, i.e., for a single molecule made of N_a atoms:

$$\mathcal{Q} = \{\mathbf{q} \in \mathbb{R}^{N_a} | \sum_i q_i = Q_{\text{tot}}\}$$

The set $\mathcal{Q}$ is a manifold, whose dimension depends on the number of constraints; for a single molecule, it is $N_a - 1$. The set of acceptable SCF densities is a so-called Grassman manifold[68]

$$\mathcal{P} = \{\mathbf{P} \in \mathbb{R}^{N_b \times N_b},\ \mathbf{P}^\dagger = \mathbf{P},\ \text{tr}\,\mathbf{P} = N,\ \mathbf{P}^2 = \mathbf{P}\}$$

where N_b is the number of basis functions (i.e., of MOs) and N is the number of electrons. Such a manifold dimension is $N(N_b - N)$, which is to be compared with the dimension of the vector space where it is embedded, i.e., N_b^2. The origin of such differences in the domains roots deeply in the different physics that originate the densities themselves: the PCM density obeys the Poisson equation, which is a variational problem *per se*, where all the regular enough densities can be accepted. The SCF density, on the other hand, obeys the laws of quantum mechanics: the fact that not every density is acceptable is very well-known, especially in the field of density functional theory, where the N-representability problem (see the book by Eschrig[99] for a detailed treatment of the problem) is one of the biggest theoretical challenges. The FQs live in an intermediate situation: they are treated as (mostly) classical charges (i.e., they do not exchange) but are not generated by a classical source: therefore, total charge constraints need to be

dx.doi.org/10.1021/ct3005062 | J. Chem. Theory Comput. XXXX, XXX, XXX−XXX

imposed. While this has few consequences from a computational point of view, the smoothness in the switching from a pure QM to a pure classical description introduced by the intermediate FQ layer is fascinating.

■ ASSOCIATED CONTENT

Supporting Information

The structure of the pyrimidine−water cluster and of the biological system in .xyz format. This material is available free of charge via the Internet at http://pubs.acs.org

■ AUTHOR INFORMATION

Corresponding Author

*E-mail: f.lipparini@sns.it.

Notes

The authors declare no competing financial interest.

■ ACKNOWLEDGMENTS

The authors would like to thank Dr. Giacomo Prampolini for providing the pyrimidine/water MD snapshots and Prof. Massimo Olivucci for providing us with the structure of the retinal−rhodopsin system and useful discussion. Dr. Giovanni Scalmani has been of invaluable help in the coding phase. The authors gratefully acknowledge financial support from Gaussian, Inc. and COST (Action CODECS: "COnvergent Distributed Environment for Computational Spectroscopy"). C.C. acknowledges support from the Italian MIUR (PRIN 2009: Sviluppo di modelli accurati e di codici veloci per il calcolo di spettri vibrazionali and FIRB-Futuro in Ricerca Protocollo: RBFR10Y5VW).

■ REFERENCES

(1) Warshel, A.; Levitt, M. *J. Mol. Biol.* **1976**, *103*, 227−249.
(2) Gao, J.; Xia, X. *Science* **1992**, *258*, 631−635.
(3) Thompson, M. A. *J. Phys. Chem.* **1996**, *100*, 14492−14507.
(4) Field, M. J.; Bash, P. A.; Karplus, M. *J. Comput. Chem.* **1990**, *11*, 700−733.
(5) Gao, J.; Freindorf, M. *J. Phys. Chem. A* **1997**, *101*, 3182−3188.
(6) Martn, M. E.; Sánchez, M. L.; del Valle, F. J. O.; Aguilar, M. A. *J. Chem. Phys.* **2000**, *113*, 6308−6315.
(7) Cui, Q.; Karplus, M. *J. Chem. Phys.* **2000**, *112*, 1133−1149.
(8) Cui, Q.; Karplus, M. *J. Phys. Chem. B* **2000**, *104*, 3721−3743.
(9) Curutchet, C.; Muñoz-Losa, A.; Monti, S.; Kongsted, J.; Scholes, G. D.; Mennucci, B. *J. Chem. Theory Comput.* **2009**, *5*, 1838−1848.
(10) Cappelli, C.; Mennucci, B.; Monti, S. *J. Phys. Chem. A* **2005**, *109*, 1933−1943.
(11) Bakowies, D.; Thiel, W. *J. Phys. Chem.* **1996**, *100*, 10580−10594.
(12) Tomasi, J.; Persico, M. *Chem. Rev.* **1994**, *94*, 2027−2094.
(13) Tomasi, J.; Mennucci, B.; Cammi, R. *Chem. Rev.* **2005**, *105*, 2999−3093.
(14) Mennucci, B. *J. Phys. Chem. Lett.* **2010**, *1*, 1666−1674 and references therein.
(15) Vreven, T.; Mennucci, B.; da Silva, C.; Morokuma, K.; Tomasi, J. *J. Chem. Phys.* **2001**, *115*, 62−72.
(16) Rega, N.; Cossi, M.; Barone, V. *J. Am. Chem. Soc.* **1998**, *120*, 5723−5732.
(17) Cui, Q. *J. Chem. Phys.* **2002**, *117*, 4720−4728.
(18) Pedone, A.; Biczysko, M.; Barone, V. *ChemPhysChem* **2010**, *11*, 1812−1832.
(19) Barone, V.; Bloino, J.; Monti, S.; Pedone, A.; Prampolini, G. *Phys. Chem. Chem. Phys.* **2010**, *12*, 10550−10561.
(20) Steindal, A. H.; Ruud, K.; Frediani, L.; Aidas, K.; Kongsted, J. *J. Phys. Chem. B* **2011**, *115*, 3027−3037.
(21) Rega, N.; Cossi, M.; Barone, V. *J. Am. Chem. Soc.* **1997**, *119*, 12962−12967.
(22) Benzi, C.; Improta, R.; Scalmani, G.; Barone, V. *J. Comput. Chem.* **2002**, *23*, 341−350.
(23) Barone, V.; Biczysko, M.; Brancato, G. In *Combining Quantum Mechanics and Molecular Mechanics. Some Recent Progresses in QM/MM Methods*; Sabin, J. R., Canuto, S., Eds.; Academic Press: New York, 2010, Vol. *59*.
(24) Thole, B. *Chem. Phys.* **1981**, *59*, 341−350.
(25) Rick, S. W.; Stuart, S. J.; Berne, B. J. *J. Chem. Phys.* **1994**, *101*, 6141−6156.
(26) Lipparini, F.; Barone, V. *J. Chem. Theory Comput.* **2011**, *7*, 3711−3724.
(27) Brancato, G.; Rega, N.; Barone, V. *J. Chem. Phys.* **2006**, *124*, 214505.
(28) Brancato, G.; Nola, A. D.; Barone, V.; Amadei, A. *J. Chem. Phys.* **2005**, *122*, 154109.
(29) Rega, N.; Brancato, G.; Barone, V. *Chem. Phys. Lett.* **2006**, *422*, 367−371.
(30) Brancato, G.; Barone, V.; Rega, N. *Theoretical Chemistry Accounts: Theory, Computation, and Modeling (Theoretica Chimica Acta)* **2007**, *117*, 1001−1015.
(31) Brancato, G.; Rega, N.; Barone, V. *J. Chem. Phys.* **2008**, *128*, 144501.
(32) Schwabe, T.; Olsen, J. M. H.; Sneskov, K.; Kongsted, J.; Christiansen, O. *J. Chem. Theory Comput.* **2011**, *7*, 2209−2217.
(33) Nielsen, C. B.; Christiansen, O.; Mikkelsen, K. V.; Kongsted, J. *J. Chem. Phys.* **2007**, *126*, 154112.
(34) Kongsted, J.; Osted, A.; Mikkelsen, K. V.; Christiansen, O. *J. Chem. Phys.* **2003**, *118*, 1620−1633.
(35) Sneskov, K.; Schwabe, T.; Christiansen, O.; Kongsted, J. *Phys. Chem. Chem. Phys.* **2011**, *13*, 18551−18560.
(36) Steindal, A. H.; Olsen, J. M. H.; Ruud, K.; Frediani, L.; Kongsted, J. *Phys. Chem. Chem. Phys.* **2012**, *14*, 5440−5451.
(37) Marini, A.; Muñoz-Losa, A.; Biancardi, A.; Mennucci, B. *J. Phys. Chem. B* **2010**, *114*, 17128−17135.
(38) Jacobson, L. D.; Herbert, J. M. *J. Chem. Phys.* **2010**, *133*, 154506.
(39) Scholes, G. D.; Curutchet, C.; Mennucci, B.; Cammi, R.; Tomasi, J. *J. Phys. Chem. B* **2007**, *111*, 6978−6982.
(40) Curutchet, C.; Kongsted, J.; Muñoz-Losa, A.; Hossein-Nejad, H.; Scholes, G. D.; Mennucci, B. *J. Am. Chem. Soc.* **2011**, *133*, 3078−3084.
(41) Rick, S. W.; Berne, B. J. *J. Am. Chem. Soc.* **1996**, *118*, 672−679.
(42) Rick, S. W.; Stuart, S. J.; Bader, J. S.; Berne, B. J. *J. Mol. Liq.* **1995**, *65−66*, 31−40.
(43) Mortier, W. J.; Van Genechten, K.; Gasteiger, J. *J. Am. Chem. Soc.* **1985**, *107*, 829−835.
(44) Chelli, R.; Procacci, P. *J. Chem. Phys.* **2002**, *117*, 9175−9189.
(45) Rappe, A.; Goddard, W. *J. Phys. Chem.* **1991**, *95*, 3358−3363.
(46) Chelli, R.; Ciabatti, S.; Cardini, G.; Righini, R.; Procacci, P. *J. Chem. Phys.* **1999**, *111*, 4218−4229.
(47) Llanta, E.; Ando, K.; Rey, R. *J. Phys. Chem. B* **2001**, *105*, 7783−7791.
(48) Llanta, E.; Rey, R. *Chem. Phys. Lett.* **2001**, *340*, 173−178.
(49) Olano, L. R.; Rick, S. W. *J. Comput. Chem.* **2005**, *26*, 699−707.
(50) Lee, A. J.; Rick, S. W. *J. Chem. Phys.* **2011**, *134*, 184507.
(51) York, D. M.; Yang, W. *J. Chem. Phys.* **1996**, *104*, 159−172.
(52) Verstraelen, T.; Speybroeck, V. V.; Waroquier, M. *J. Chem. Phys.* **2009**, *131*, 044127.
(53) Chelli, R.; Pagliai, M.; Procacci, P.; Cardini, G.; Schettino, V. *J. Chem. Phys.* **2005**, *122*, 074504.
(54) Nishimoto, K.; Mataga, N. Z. *Phys. Chem. (Frankfurt)* **1957**, *12*, 335.
(55) Ohno, K. *Theor. Chem. Acc.* **1964**, *2*, 219−227.
(56) Louwen, J. N.; Vogt, E. T. C. *J. Mol. Catal. A: Chem.* **1998**, *134*, 63−77.
(57) Patel, S.; Brooks, C. *J. Comput. Chem.* **2004**, *25*, 1−15.
(58) Patel, S.; Mackerell, A.; Brooks, C. *J. Comput. Chem.* **2004**, *25*, 1504−1514.
(59) van Duin, A. C. T.; Dasgupta, S.; Lorant, F.; Goddard, W. A. *J. Phys. Chem. A* **2001**, *105*, 9396−9409.

(60) Chen, J.; Martinez, T. J. *Chem. Phys. Lett.* **2008**, *463*, 288.
(61) Nistor, R. A.; Polihronov, J. G.; Müser, M. H.; Mosey, N. J. *J. Chem. Phys.* **2006**, *125*, 094108.
(62) Verstraelen, T.; Bultinck, P.; Van Speybroeck, V.; Ayers, P. W.; Van Neck, D.; Waroquier, M. *J. Chem. Theory Comput.* **2011**, *7*, 1750−1764.
(63) Ando, K. *J. Chem. Phys.* **2001**, *115*, 5228−5237.
(64) Lipparini, F.; Scalmani, G.; Mennucci, B.; Cancès, E.; Caricato, M.; Frisch, M. J. *J. Chem. Phys.* **2010**, *133*, 014106.
(65) Lipparini, F.; Scalmani, G.; Mennucci, B.; Frisch, M. J. *J. Chem. Theory Comput.* **2011**, *7*, 610−617.
(66) Pulay, P. *Chem. Phys. Lett.* **1980**, *73*, 393−398.
(67) Pulay, P. *J. Comput. Chem.* **1982**, *3*, 556−560.
(68) Kudin, K. N.; Cancès, E.; Scuseria, G. E. *J. Chem. Phys.* **2002**, *116*, 8255−8261.
(69) Vreven, T.; Byun, K. S.; Komaromi, I.; Dapprich, S.; Montgomery, J. A. J.; Morokuma, K.; Frisch, M. J. *J. Chem. Theory Comput.* **2006**, *2*, 815−826.
(70) Dapprich, S.; Komaromi, I.; Byun, K.; Morokuma, K.; Frisch, M. *J. Mol. Struct.: THEOCHEM* **1999**, *461*, 1−21.
(71) Klamt, A.; Schuurmann, G. *J. Chem. Soc., Perk. Trans. 2* **1993**, 799−805.
(72) Barone, V.; Cossi, M. *J. Phys. Chem. A* **1998**, *102*, 1995−2001.
(73) Cossi, M.; Rega, N.; Scalmani, G.; Barone, V. *J. Comput. Chem.* **2003**, *24*, 669−681.
(74) Scalmani, G.; Barone, V.; Kudin, K.; Pomelli, C.; Scuseria, G.; Frisch, M. *Theor. Chem. Acc.* **2004**, *111*, 90−100.
(75) Cancès, E. In *Continuum Solvation Models in Chemical Physics*; Mennucci, B.; Cammi, R., Eds.; Wiley, New York: 2007; Chapter 1.2, pp 29−48.
(76) Cossi, M.; Scalmani, G.; Rega, N.; Barone, V. *J. Chem. Phys.* **2002**, *117*, 43−54.
(77) Scalmani, G.; Frisch, M. J. *J. Chem. Phys.* **2010**, *132*, 114110.
(78) Mahoney, M. W.; Jorgensen, W. L. *J. Chem. Phys.* **2000**, *112*, 8910−8922.
(79) Cammi, R.; Tomasi, J. *Int. J. Quantum Chem.* **1995**, *56*, 465−474.
(80) Mennucci, B. In *Continuum Solvation Models in Chemical Physics*; Mennucci, B., Cammi, R., Eds.; Wiley: New York, 2007; Chapter 1.5, pp 110−124.
(81) Mennucci, B.; Cappelli, C.; Guido, C. A.; Cammi, R.; Tomasi, J. *J. Phys. Chem. A* **2009**, *113*, 3009−3020.
(82) Mennucci, B.; Cappelli, C.; Cammi, R.; Tomasi, J. *Theor. Chem. Acc.* **2007**, *117*, 1029−1039.
(83) Casida, M. E.; Jamorski, C.; Casida, K. C.; Salahub, D. R. *J. Chem. Phys.* **1998**, *108*, 4439−4449.
(84) Yanai, T.; Tew, D.; Handy, N. *Chem. Phys. Lett.* **2004**, *393*, 51−57.
(85) Barone, V.; Cimino, P.; Stendardo, E. *J. Chem. Theory Comput.* **2008**, *4*, 751−764.
(86) Double- and triple-ζ basis sets of the n07 family are available for download. Visit http://idea.sns.it (accessed June 5, 2012).
(87) Karelson, M. M.; Zerner, M. C. *J. Phys. Chem.* **1992**, *96*, 6949−6957.
(88) Karelson, M.; Zerner, M. C. *J. Am. Chem. Soc.* **1990**, *112*, 9405−9406.
(89) Gao, J.; Byun, K. *Theor. Chem. Acc.* **1997**, *96*, 151−156.
(90) Becke, A. *J. Chem. Phys.* **1993**, *98*, 5648−5652.
(91) Jorgensen, W. L.; Chandrasekhar, J.; Madura, J. D.; Impey, R. W.; Klein, M. L. *J. Chem. Phys.* **1983**, *79*, 926−935.
(92) Biczysko, M.; Bloino, J.; Brancato, G.; Cacelli, I.; Cappelli, C.; Ferretti, A.; Lami, A.; Monti, S.; Pedone, A.; Prampolini, G.; Puzzarini, C.; Santoro, F.; Trani, F.; Villani, G. *Theor. Chem. Acc.* **2012**, *131*, 1−19.
(93) Magyar, R. J.; Tretiak, S. *J. Chem. Theory Comput.* **2007**, *3*, 976−987.
(94) Huntress, M. M.; Gozem, S.; Malley, K. R.; Jailaubekov, A. E.; Vasileiou, C.; Vengris, M.; Geiger, J. H.; Borhan, B.; Schapiro, I.; Larsen, D. S.; Olivucci, M. Photophysics of the Retinal Chromophore in a Rhodopsin Mimic. Submitted to *J. Phys. Chem. B* for publication.
(95) Cancès, E.; Mennucci, B.; Tomasi, J. *J. Chem. Phys.* **1997**, *107*, 3032−3041.
(96) Cancès, E.; Mennucci, B. *J. Math. Chem.* **1998**, *23*, 309−326.
(97) Jordanides, X. J.; Lang, M. J.; Song, X.; Fleming, G. R. *J. Phys. Chem. B* **1999**, *103*, 7995−8005.
(98) Cornell, W.; Cieplak, P.; Bayly, C.; Gould, I.; Merz, K.; Ferguson, D.; Spellmeyer, D.; Fox, T.; Caldwell, J.; Kollman, P. *J. Am. Chem. Soc.* **1995**, *117*, 5179−5197.
(99) Eschrig, H. *The Fundamentals of Density Functional Theory*; Edition am Gutenbergplatz: Leipzig, Germany, 2003.